JOURNAL OF VIROLOGY, Feb. 1994, p. 863–876
0022-538X/94/$04.00+0

Vol. 68, No. 2

Clustered Charged-to-Alanine Mutagenesis of Poliovirus RNA-Dependent RNA Polymerase Yields Multiple Temperature-Sensitive Mutants Defective in RNA Synthesis

SCOTT E. DIAMOND AND KARLA KIRKEGAARD*

Department of Molecular, Cellular and Developmental Biology and Howard Hughes Medical Institute, University of Colorado, Boulder, Colorado 80309-0347

Received 29 June 1993/Accepted 29 October 1993

To generate a collection of conditionally defective poliovirus mutants, clustered charged-to-alanine mutagenesis of the RNA-dependent RNA polymerase 3D was performed. Clusters of charged residues in the polymerase coding region were replaced with alanines by deoxyoligonucleotide-directed mutagenesis of a full-length poliovirus cDNA clone. Following transfection of 27 mutagenized cDNA clones, 10 (37%) gave rise to viruses with temperature-sensitive (*ts*) phenotypes. Three of the *ts* mutants displayed severe *ts* plaque reduction phenotypes, producing at least 10^3-fold fewer plaques at 39.5°C than at 32.5°C; the other seven mutants displayed *ts* small-plaque phenotypes. Constant-temperature, single-cycle infections showed defects in virus yield or RNA accumulation at the nonpermissive temperature for eight stable *ts* mutants. In temperature shift experiments, seven of the *ts* mutants showed reduced accumulation of viral RNA at the nonpermissive temperature and showed no other *ts* defects. The mutations responsible for the phenotypes of most of these *ts* mutants lie in the N-terminal third of the 3D coding region, where no well-characterized mutations responsible for viable mutants had been previously identified. Clustered charged-to-alanine mutagenesis (S. H. Bass, M. G. Mulkerrin, and J. A. Wells, Proc. Natl. Acad. Sci. USA 88:4498–4502, 1991; W. F. Bennett, N. F. Paoni, B. A. Keyt, D. Botstein, J. J. S. Jones, L. Presta, F. M. Wurm, and M. J. Zoller, J. Biol. Chem. 266:5191–5201, 1991; and K. F. Wertman, D. G. Drubin, and D. Botstein, Genetics 132:337–350, 1992) is designed to target residues on the surfaces of folded proteins; thus, extragenic suppression analysis of such mutant viruses may be very useful in identifying components of the viral replication complex.

RNA-dependent RNA polymerases are required by all RNA viruses, except retroviruses, for replication of their genomes. In cases for which template specificity for the viral RNA has been reconstituted in vitro, the RNA-dependent RNA polymerases have been found to function in replicase complexes (31, 77) containing other viral or host proteins. Qβ replicase activity requires a phage-encoded protein and three proteins from its *Escherichia coli* host: translational elongation factors EF-Tu and EF-Ts, as well as ribosomal protein S1 (15, 74). Template-specific negative-strand synthesis by the *Saccharomyces cerevisiae* double-stranded RNA virus L-A occurs only within the intact capsid (26). For brome mosaic virus, a template-specific replicase complex was found to contain a subunit of translation initiation factor eIF-3 (54).

Nevertheless, enzymatic function appears to reside within virally encoded proteins, some of which display nonspecific RNA-dependent RNA polymerase activity in isolation (25, 51, 59, 73) and all of which have sequence similarity in at least four regions of the primary sequence (16, 38, 53). Two of these conserved regions are also shared by DNA- and RNA-dependent DNA polymerases (23), and one of the regions of conserved sequence, containing a highly conserved YGDD motif, may be related to the YGDTD sequence conserved among DNA-dependent DNA polymerases (5). Mutagenesis of these conserved regions has usually resulted in nonviable viruses and polymerases which display greatly reduced specific activity in vitro (32, 33, 49, 58, 59, 69). None of the mutant viruses has been shown to display a conditional phenotype such as heat or cold sensitivity, which would facilitate investigation of the altered in vivo function.

Poliovirus, a positive-strand RNA virus that infects primate cells, is a member of the family *Picornaviridae*. Its 7,500-nucleotide (nt) single-stranded RNA genome contains one open reading frame encoding a single 247-kDa polyprotein. This polyprotein is proteolytically processed into a number of viral polypeptides (42), one of which, 3D, displays RNA-dependent RNA polymerase activity in vitro (73). The 461-amino-acid sequence of 3D (42, 56) contains the consensus sequences for RNA-dependent RNA polymerases (16, 38, 53). Yet 3D polymerase, while able to elongate RNA chains, has shown no ability either to initiate RNA synthesis independently or to provide the specificity for such synthesis in vitro (22, 71). It is likely that other viral and possibly cellular proteins form, with the polymerase, a replication complex capable of both initiating RNA synthesis and achieving specificity of RNA replication.

Progress has been made in identifying the viral components of such a replication complex (13, 62). The viral protein 3B (VPg) is covalently attached to the 5′ ends of poliovirus RNA strands and may act as part of the priming mechanism in vivo (62). Mutational analyses have implicated the poliovirus coding regions 2B, 2C, 3A, 3B, 3C, and 3D, as well as the 3′ and 5′ noncoding regions, in poliovirus RNA replication: mutations at each of these loci have been shown to cause primary defects in RNA replication (1, 3, 9, 19, 28, 36, 46, 57, 61, 70). The polypeptide products of the coding regions 2B, 2C, 3A, 3B, and 3D, along with newly synthesized poliovirus RNA, were found to colocalize to the cytoplasmic surfaces of virally induced membranous vesicles (11–13). Recently, the entire

* Corresponding author. Mailing address: Department of Molecular, Cellular and Developmental Biology, Howard Hughes Medical Institute, University of Colorado, Campus Box 347, Boulder, CO 80309-0347. Phone: (303) 492-7882. Fax: (303) 492-7576.

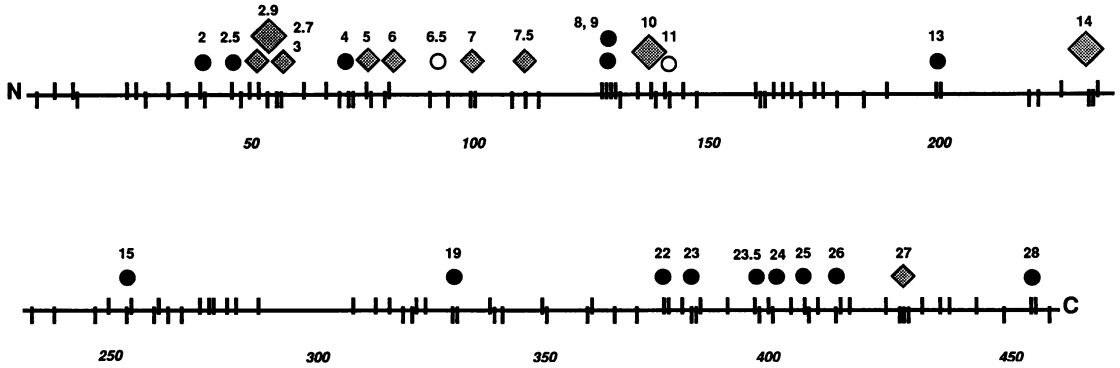

FIG. 1. Schematic representation of the 461-amino-acid sequence of 3D, the poliovirus RNA-dependent RNA polymerase, showing the locations of charged residues and clustered charged-to-alanine mutations. The locations of acidic residues are shown by short vertical slashes below the horizontal line that represents the 461-amino-acid sequence; basic residues are shown by slashes above the line. The locations of the clustered charged-to-alanine mutations that were introduced and the plaque phenotypes of resulting mutant viruses are shown as follows: ○, mutant virus displayed wild-type phenotype; ●, no mutant virus was recovered; ◈, *ts* virus with a plaque reduction phenotype was recovered; ◈, *ts* virus with a small-plaque phenotype was recovered. Mutant AL-14 contains an additional single-nucleotide substitution, leading to the substitution of cysteine for tyrosine at amino acid 264.

intracellular poliovirus replicative cycle, including virus RNA-specific positive- and negative-strand synthesis, has been shown to occur in vitro, programmed by RNA transcripts (6, 50). These in vitro reactions contain cellular membranous structures and are extremely sensitive to treatment with nonionic detergents (49a), further supporting the idea that poliovirus-specific RNA synthesis requires membrane-associated complexes.

In addition to their presumed function in both positive- and negative-strand viral RNA synthesis, 3D sequences can also function as part of the fusion protein 3CD. The 3CD polypeptide is known to function as a protease, whose specificity differs from that of the 3C protease alone (14, 37, 78). In addition, 3CD protein has been shown to bind specifically, in a complex with a 36-kDa host cell protein, to RNA sequences at the 5′ end of the poliovirus positive strand (3).

Conditional mutants bearing mutations in the 3D coding region that display specific defects in RNA replication would be useful in the identification of 3D residues that are required for the different functions of 3D and, possibly, for the interactions between 3D and other viral and cellular proteins. Because of the high error rate of RNA-dependent RNA polymerases (64, 65, 75), single-nucleotide substitutions are often genetically unstable; more extensive genetic changes often result in nonviable viruses (17). Thus, despite considerable effort from several laboratories, only five well-defined mutations in the 3D coding region (see Fig. 7) that give rise to viable virus with measurable phenotypic defects have been reported (10, 18, 19). Mutagenesis of one residue in 3D, Asn-424, has yielded three of these mutants; viruses containing alterations in Asn-424 were found to be temperature sensitive (*ts*) and to encode polymerases that were not defective for RNA elongation in vitro (1, 18). A *ts* mutant caused by the insertion of a single leucine residue between amino acids 257 and 258 of 3D was shown, in temperature shift experiments, to display specific defects in both RNA synthesis and proteolytic processing of viral capsid proteins at the nonpermissive temperature (19). In this case, the mutant polymerase was defective for RNA elongation in vitro (19). A small-plaque poliovirus mutant, whose nonconditional mutant phenotype was caused by insertion of a single threonine residue between amino acids 354 and 355 of 3D, displayed delayed RNA synthesis (10).

A mutagenesis algorithm termed clustered charged-to-alanine mutagenesis was originally used to investigate the role of surface charges in the functions of two proteins, the human growth hormone receptor (7) and *S. cerevisiae* cyclic AMP-dependent protein kinase (29). The resulting alleles displayed interesting in vitro phenotypes: many seem to disrupt important intermolecular contacts. For example, clustered charged-to-alanine mutagenesis of the human growth hormone receptor allowed the identification of clusters of charged residues that are required for hormone binding (7). Recently, a high proportion of mutations introduced into the *S. cerevisiae* actin gene, *ACT1*, using this algorithm, were shown to give rise to *S. cerevisiae* that was *ts* in vivo (76). Specifically, 44% of the mutant alleles were shown to confer *ts* phenotypes to yeast cells.

Why should charged-residue-to-alanine mutations cause such a high proportion of mutants with *ts* phenotypes? Single substitutions of charged residues with alanine in other proteins have generally been shown to exert little effect on protein conformation but instead to interfere with specific in vitro activities (20, 39, 68). Most charged residues, especially those found in clusters in the primary sequence of proteins, are expected to reside on the solvent-exposed surfaces of folded proteins (20, 76) and to contribute little to overall protein stability (21). Disruption of such clusters of surface charge might not disrupt overall protein stability but instead might interfere with electrostatic or hydrogen-bonding interactions with other biomolecules or with the solvent, making these interactions more thermosensitive (2, 76).

To obtain a collection of *ts* mutants containing mutations in the 3D coding region and to test the utility of this technique in another protein besides actin, we constructed 27 clustered charged-to-alanine mutations in the 3D RNA-dependent RNA polymerase coding region of Mahoney type 1 poliovirus. Nine of these sets of mutations conferred *ts* phenotypes to the mutant polioviruses; seven of these displayed specific defects in viral RNA synthesis in temperature shift experiments. These new conditional alleles define new locations in the 3D coding region and should prove useful in disrupting specific steps of RNA replication and, possibly, in disrupting specific interactions between the polymerase and other components of the replication complex.

MATERIALS AND METHODS

Cells and viruses. Wild-type Mahoney type 1 poliovirus used in these experiments was derived from a single plaque that resulted from transfection of the infectious viral cDNA (55) present in a plasmid termed pMlu, a derivative of pPolio (41). The nomenclature for viral mutants suggested by Bernstein et al. (10) was employed.

HeLa cells were grown either in suspension in minimal essential medium (Joklik modification) supplemented with 7% horse serum (GIBCO Laboratories) or in petri dishes in Dulbecco modified Eagle medium supplemented with 10% calf serum (GIBCO). High-titer virus stocks were prepared by infecting HeLa cells in petri dishes (Corning) at 37°C for wild-type poliovirus and at 32.5°C for mutant polioviruses. Plaque assays were performed as described previously (40). Incubations under agar at 37 and 39.5°C were continued for 48 h, and those at 32.5°C were continued for 72 h.

Construction of mutant plasmids. To create subclones of 3D-encoding poliovirus sequences suitable for site-directed mutagenesis, pMlu DNA was digested with *Bgl*II, *Pvu*II, and *Eco*RI (New England Biolabs), and segments of poliovirus type 1 (Mahoney) corresponding to nt 5601 to 7053, 7053 to 7512, or 5601 to 7512 were subcloned into pBluescript KS+ DNA (Stratagene) by utilizing appropriate *Bgl*II, *Eco*RI and *Pvu*II sites.

The new plasmids, pBSKS+5601−7053, pBSKS+7053−7512, and pBSKS+5601−7512, were transformed into CJ236 (*ung dut* Cam^r), and dU-containing single-strand phagemid DNA was prepared according to the commercial protocol (Stratagene) with the following modifications: phagemid particles were pelleted from the clarified supernatant only after addition of polyethylene glycol to 5% and NaCl to 0.5 M and incubation on ice for 30 min.

Deoxyoligonucleotide mutagenesis was performed according to the method of Kunkel (43), except that the Klenow fragment of *E. coli* polymerase I (N.E.B.) was used instead of T4 polymerase. Twenty-seven clustered charged-to-alanine mutations were constructed by using the following negative-sense deoxyoligonucleotides synthesized by J. Binkley (University of Colorado). In the sequences of the mutagenic deoxyoligonucleotides given below, sequences complementary to the introduced alanine codons are underlined and the nucleotides that differ from the sequence of the poliovirus negative strand are shown in boldface. Each set of mutations created a novel *Bst*UI (CGCG) restriction endonuclease site. The mutagenic deoxyoligonucleotides used were as follows: GGACTGCTG G**CGCGGC**CACCCCTTCA (AL-2); CTGTCTTAAG**CGC**G GG**TGC**GTTTTTAGTG (AL-2.5); CCTCCTCAAA**CGCG** GT**CGC**AAGCCTGGGA (AL-2.7); AGAAAATTGC**CGCG** **GC**AAA**GGC**TGTCTTAAGC (AL-2.9); AGAAAATTGC **CGCGGC**AAAGTCTGTC (AL-3); CTTTCATGTA**CGCGG** **C**CACTTCAGTA (AL-4); GGTCTACTGC**CGCGGC**CATG TACTCA (AL-5); GGCCAGCATA**CGCGGC**TACTGCCT CT (AL-6); AGCACATTTG**CGC**GGTGTTGAT**GGC**TAG TGACATG (AL-6.5); CATACATGGC**CGCGGC**CAAGC ACATT (AL-7); AATCAAGTGC**CGC**GAGACC**AGC**AGT GCCATAC (AL-7.5); AGATGTCTCT**CGCCGCGGC**TC CCATTGCT (AL-8); TGTTCAAGAT**CGCGGCCGC**CTTC TTTCCC (AL-9); TTTCCTTAGT**CGCGGC**GGTTTGTTTG (AL-10); GTTTTTGCAT**CGCGGC**AGT GTCTCTG (AL-11); CTCCTGGGTT**CGCGGC**AAAAGCAGCA (AL-13); CAAACAGCTT**CGCGGC**CATCAATACC (AL-14); CGAA TCCGAT**CGCGGC**AAGCACCATC (AL-15); AAGCAA TTAC**CGCGGC**ACCATAGGCA (AL-19); CCCTGAAGAA **CGCGGC**CAAGAATGTT (AL-22); GAAATGGGTA**TGC** **CGCGGC**TGCCCTGAAG (AL-23); ATTCATGAAT**CGCG** **GC**CATTGGCATT (AL-23.5); ATCTAATTGA**CGCGGC**A ATTTCCTTC (AL-24); TGTTCCTAGG**CGCGGC**AGTCC ATCTA (AL-25); GAGAGCGAAC**CGCGGC**CTGAGTG TTC (AL-25); ATTTGTTATA**TGCCGCGGC**GCCATTG TGC (AL-27); and AGTCAAGCCA**CGCGGC**GTACAAT GTT (AL-28). The presence of the introduced mutations was tested by digestion with *Bst*UI. The 3D-encoding sequences of each mutagenized plasmid were excised by digestion with *Bgl*II and *Pvu*II or with *Pvu*II and *Eco*RI and cloned into the infectious poliovirus cDNA clone pMluN. pMluN was constructed from pMlu by the insertion of a *Not*I linker into a *Pvu*II site in the vector sequences, rendering the *Pvu*II site at nt 7053 in the poliovirus genome unique.

Screening for *ts* poliovirus mutants. Transfections of DNA were performed at 37°C with cationic liposomes according to the Lipofectin (GIBCO) protocol. Plates were subsequently overlaid with Dulbecco modified Eagle medium containing 1% agar prior to incubation at 32.5°C. From each DNA transfection that gave rise to viral plaques, five well-isolated plaques were isolated and screened individually by plaque assay. Phenotypes of high-titer stocks derived from these plaque isolates were confirmed by plaque assay.

Sequence verification of plasmids. For each mutant cDNA that gave rise to *ts* virus, the entire region that was derived from the pBluescript mutagenesis vectors was sequenced, using reagents and protocols obtained from a commercial kit (Sequenase; U.S. Biochemicals). Commercially synthesized deoxyoligonucleotides (Macromolecular Resources) contained the following sequences: CTGCTCTGGTTGGAAAGTTG, complementary to poliovirus positive-strand nt 5851 to 5870; TCAAACACATAGTGGAAAGC, complementary to positive-strand nt 6071 to 6090; CCCATTGCTACATAAGGGTA, complementary to positive-strand nt 6338 to 6357; TGTGAA AAGCAGCATATAGG, complementary to positive-strand nt 6565 to 6583; TTGTACAGGTGGTGTGAGTG, complementary to positive-strand nt 6794 to 6813; GTTACATTCTC CCATGTGAC, complementary to positive-strand nt 7082 to 7101; ACTCAGGATCACGTTCGCTC, identical to positive-strand nt 7214 to 7233; and CTCCGAATTAAAGA, complementary to positive-strand nt 7427 to 7440.

Sequence verification of virus. For each *ts* virus, the presence of the intended mutations in the mutant viral RNAs was confirmed by sequence analysis. Virus RNA purification, cDNA synthesis, and PCR from the cDNA were performed as described previously (35). DNA sequencing of the PCR products was performed as described above, except that primer-template annealing was performed by freezing on dry ice. Commercially synthesized deoxyoligonucleotides (Macromolecular Resources) contained the following sequences: AGT CAAGTCGACCATGGGTGAAATCCAGTGG, the 3′-terminal 15 nucleotides of which are identical to positive-strand nucleotides 5987 to 6001, and TGAGCCCGGGTTACTA AAATGAGTC, whose 3′-terminal 20 nucleotides are complementary to positive-strand nucleotides 7361 to 7380.

Constant-temperature infections. HeLa cells were grown in suspension to a density of 4.0×10^5 cells per ml. For each infection, approximately 2×10^8 cells were pelleted by low-speed centrifugation, resuspended in 2 ml of phosphate-buffered saline (PBS), and infected with wild-type or mutant virus at a multiplicity of infection (MOI) of 50 PFU per cell. After 30 min of viral adsorbtion at room temperature, cells were washed twice with PBS, resuspended in 50 ml of minimal essential medium supplemented with 10% fetal calf serum (GIBCO), split into two fractions, and incubated with stirring at 32.5 or 39.5°C. After 60 min, HEPES (*N*-2-hydroxyeth-

ylpiperazine-*N'*-2-ethanesulfonic acid) (pH 7.5) was added to 15 mM. At the indicated times, 2-ml samples were removed, and the cells were collected by low-speed centrifugation and washed once with PBS. The cells in one half of each sample were lysed by freezing and thawing three times, cytoplasmic extracts were prepared by centrifugation at 1,600 × *g* for 10 min at 4°C, and plaque assays were performed at 32.5°C. The cells in the other half of each sample were collected by low-speed centrifugation, total cytoplasmic RNA was prepared, and viral positive-stranded RNA was quantified as described previously (35). The amount of radioactive negative-strand probe hybridized to each sample was determined by a radioanalytic scanner (Ambis Systems); standard curves for each set of experiments were prepared to ensure that each measurement fell within the linear range of the assay (35).

Temperature shift experiments. To measure the accumulation of viral proteins, monolayers of HeLa cells in 60-mm dishes were infected with wild-type or mutant poliovirus at an MOI of 25 PFU per cell. At 7 h postinfection at 32.5°C, cells were labeled with [^{35}S]methionine (48), and incubation was continued at either 32.5 or 39.5°C for 15 min as described previously (41). Equal amounts of radioactivity from each supernatant were analyzed by electrophoresis in sodium dodecyl sulfate–12.5% polyacrylamide gels as described previously (44). In addition, 25-ml samples of supernatants were precipitated with 10% trichloroacetic acid and filtered through nitrocellulose; the amount of precipitated radioactivity was determined by liquid scintillation counting.

To analyze the processing and stability of viral proteins that were labeled at the permissive temperature, infections with wild-type and mutant viruses were performed as described above except that the 15-min labeling with [^{35}S]methionine was performed at 32.5°C. Labeled medium was removed, the plates were washed, label-free medium containing excess unlabeled methionine was added, and incubation was continued either for 90 min at 32.5°C or for 60 min at 39.5°C. Cells were harvested, and radioactive proteins were analyzed by sodium dodecyl sulfate-polyacrylamide gel electrophoresis (SDS-PAGE) as described above.

RNA accumulation was measured by performing infections with wild-type and mutant polioviruses at MOIs of 25 PFU per cell as described above. After 4 h of incubation at 32.5°C, half of the plates were shifted to 39.5°C and incubation was continued. Cells on individual plates were harvested at various times postshift and collected by low-speed centrifugation, total cytoplasmic RNA was prepared, and viral positive-stranded RNA was quantified by dot blot analysis as described previously (35).

Bacterial expression. For bacterial expression studies, wild-type and mutant pMluN plasmids were digested with *Bst*BI and *Pvu*II, and the DNA fragments corresponding to nt 6010 to 7053 of the poliovirus sequence were cloned individually into pT5T-3D, replacing the wild-type 3D sequences present in that plasmid. pT5T-3D was a gift of T. Jarvis (Ribozyme Products, Inc.) and is similar to the bacterial expression plasmid used by Plotch et al. to express 3D polymerase in *E. coli* (52). The gene expression system of Studier and Moffatt was utilized to visualize plasmid-encoded proteins (66, 67). After induction with IPTG (isopropyl-β-D-thiogalactopyranoside) for 15 min at 37°C, rifampin was added to 200 μg/ml and incubation was continued at 42°C for 5 min. Cultures were then incubated at 37°C for 20 min and labeled with [^{35}S]methionine for 5 min. Cells were washed, collected by centrifugation, and resuspended and heated in Laemmli sample buffer. Labeled proteins were displayed by SDS-PAGE as described previously (44).

RNA transfection. Mutant 3D-107 and 3D-112 pMluN plasmids were digested with *Bgl*II and *Eco*RI, and the DNA fragments corresponding to nt 5601 to 7512 of the poliovirus sequence were cloned individually into T7-pGEM-polio, replacing the wild-type 3D sequences present in that plasmid. T7-pGEM-polio is similar to T7-polio (60, 72). Wild-type and mutant full-length infectious transcripts produced from *Eco*RI-linearized plasmids were introduced into HeLa monolayers by transfection (30) with cationic liposomes (GIBCO). Plates were subsequently overlaid with Dulbecco modified Eagle medium supplemented with 10% calf serum (GIBCO) and incubated either at 32.5°C for 6 h or at 39.5°C for 4 h. Plates were washed once with PBS, and monolayers were harvested into 1 ml of PBS. The cells in each sample were lysed by freezing and thawing three times, cytoplasmic extracts were prepared by centrifugation at 1,600 × *g* for 10 min at 4°C, and plaque assays were performed at 32.5°C.

Statistical calculations. The estimate of the standard deviation of the parental population was calculated as $s = \sqrt{[\Sigma(x_i - x_{av})^2]/(n-1)}$. Most experiments were done in duplicate, and $n = 2$. In determining the ratios of two independent variables, the relative errors were added in quadrature to determine the standard deviation of the ratio z_{av}: $s_z = z_{av}\sqrt{(s_x/x_{av})^2 + (s_y/y_{av})^2}$, where $z_{av} = x_{av}/y_{av}$. The Student *t* test of the difference between two sample means was performed: $t = (x_{av} - y_{av})/\sqrt{(s_1^2/n_1) + (s_2^2/n_2)}$ with two degrees of freedom.

RESULTS

Clustered charged-to-alanine mutagenesis of 3D coding region. The goal of these experiments was to generate a collection of *ts* mutants of 3D, the poliovirus RNA-dependent RNA polymerase. To this end, clusters of two or three charged residues throughout the 3D coding region were changed sequentially to alanine, much as described by Wertman et al. (76). Specifically, any sequence of five amino acids containing two or more charged residues was a candidate to have each charged residue changed to alanine. Figure 1 shows the locations of each charged residue in the 461-amino-acid coding region of 3D and of the 27 clustered charged-to-alanine mutations that were introduced. Because of the size of the 3D coding region, all possible mutations according to the algorithm of Wertman et al. (76) were not constructed.

The nucleotide and amino acid changes for each clustered charged-to-alanine mutation are given in Table 1. Mutations were introduced by deoxyoligonucleotide-directed mutagenesis (43) of segments of the 3D coding region present in phagemid vectors; each clustered charged-to-alanine mutation also created a novel *Bst*UI restriction endonuclease site to facilitate screening for introduced mutations (see Materials and Methods). Each of the clustered charged-to-alanine mutations was subsequently transferred to a full-length, otherwise wild-type poliovirus cDNA clone. Mutated full-length cDNAs were introduced into HeLa monolayers at 32.5 and 39.5°C by cationic liposome-mediated transfection, and the monolayers were overlaid with agar. Twelve of the mutated cDNAs gave rise to plaques after incubation at 32.5°C.

***ts* plaque phenotypes of 10 mutant viruses resulting from clustered charged-to-alanine mutagenesis.** The plaque phenotypes of the 12 viable mutant viruses were determined to identify those that were *ts*. From each 32.5°C DNA transfection, five individual plaques were isolated, and the titers of viruses derived from each of the plaques were determined at both 32.5 and 39.5°C on HeLa monolayers. Viruses from

TABLE 1. Clustered charged-to-alanine mutations

Original designation	Nucleotides changed	Residues changed to alanine	Plaque phenotype of virus at:		Designation of mutant virus
			32.5°C	39.5°C	
AL-2	A6098G, A6099C, G6100C, A6102C, A6103G	K38, E39	—[a]	—	
AL-2.5	A6126C, T6127A, A6131G, G6132C	D47, R49	—	—	
AL-2.7	A6137G, A6138C, A6142C, A6144C, C6145G	K51, D53	Wild type	Small plaques (25 to 50% of wild-type diameter)	3D-106
AL-2.9	A6144C, A6150C, G6151C, A6153C	D53, E55, E56	Wild type	1,000 times fewer plaques	3D-107
AL-3	A6150C, G6151C, A6153C	E55, E56	Wild type	Small plaques (50 to 80% of wild-type diameter)	3D-108
AL-4	A6198C, T6199C, A6201C	D71, E72	—	—	
AL-5	A6209G, A6210C, A6211C, A6213C	K75, E76	Wild type	Small plaques (25 to 50% of wild-type diameter)	3D-109
AL-6	A6222C, C6224G, A6225C, C6226G	D79, H80	Wild type	Small plaques (25 to 50% of wild-type diameter)	3D-110
AL-6.5	A6252C, A6262C, A6264C, A6265G	D89, E93	Wild type	Wild type	
AL-7	A6279C, G6280C, A6282C, T6283G	E98, D99	Wild type	Small plaques (25 to 50% of wild-type diameter)	3D-111
AL-7.5	A6300C, A6309C, A6310G	D105, E108	Small plaques (25 to 50% of wild-type diameter)	Small plaques (<25% of wild-type diameter)	
AL-8	A6359G, A6360C, G6361C, A6362G, A6363C, A6365G, A6366C	K125, K126, K127	—	—	
AL-9	A6365G, A6366C, AA6368G, G6369C, A6370C, A6372C, C6373G	K127, R128, D129	—	—	
AL-10	A6392G, G6393C, A6394C, A6396C, C6397G	R136, D137	Wild type	1,000 times fewer plaques	3D-112
AL-11	A6401G, A6402C, G6403C, A6405C, A6406G	K139, E140	Wild type	Wild type	
AL-13	C6581G, A6582C, A6584G, A6585C, A6586G	H149, K150	—	—	
AL-14[b]	A6663C, A6664C, A6666C	E226, E227	Small plaques (50 to 80% of wild-type diameter)	1,000 times fewer plaques	3D-113
AL-15	A6747C, G6748C, A6749G, A6750C, A6751G	E254, K255	—	—	
AL-19	A6969C, T6970C, A6972C, T6973G	D328, D329	—	—	
AL-22	A7109G, A7110C, G7111C, A7112G, G7113C, A7114G	K375, R376	—	—	
AL-23	A7128C, A7131C, A7133G, A7134C	D381, E382, K383	—	—	
AL-23.5	A7169G, A7170C, G7171C, A7173C, A7174G	K395, E396	—	—	
AL-24	C7178G, A7179C, T7180C, A7182C, A7183G	H398, E399	—	—	
AL-25	A7199G, A7200C, A7201C, A7203C, T7204G	K405, D406	—	—	
AL-26	A7221C, T7222C, C7223G, A7224C, C7225G	D412, H413	—	—	
AL-27	A7263C, A7264C, A7266C, A7267G, A7269C	E426, E427, E428	Wild type	Small plaques (<25% of wild-type diameter)	3D-114
AL-28	C7349G, G7350C, C7352G, G7353C, T7354GO	R455, R456	—	—	

[a] —, does not produce virus when introduced into HeLa cells by transfection.
[b] An additional nucleotide change, A6777G, resulted in amino acid substitution Y264C.

plaque isolates from the same mutant cDNA behaved identically in every case. The results of these plaque assays are summarized in Fig. 1 and Table 1. Viruses obtained from transfection of AL-6.5 and AL-11 cDNAs displayed wild-type plaque phenotypes and were not characterized further. The remaining 10 viable mutant viruses exhibited *ts* plaque phenotypes (Table 1). Seven of these *ts* mutant viruses formed the same number of plaques at 39.5 as at 32.5°C, but the plaques formed at the higher temperature were distinctly smaller. One of these *ts* small-plaque mutants, derived from AL-7.5 cDNA, also formed small plaques at 32.5°C and was quite unstable phenotypically; this virus was not characterized further. The remaining three *ts* mutant viruses displayed severe *ts* plaque reduction phenotypes, forming 1,000-fold fewer plaques at 39.5 than at 32.5°C (Table 1). Thus, a high yield of *ts* mutants that displayed both plaque reduction and small-plaque *ts* phenotypes was obtained from the clustered charged-to-alanine mutagenesis.

The nine stable *ts* mutant viruses were named (Table 1) to conform with recommended nomenclature (10): the *ts* plaque reduction mutants were designated 3D-107, 3D-112, and 3D-113, and the *ts* small-plaque mutants were designated 3D-106, 3D-108, 3D-109, 3D-110, 3D-111, and 3D-114. High-titer stocks of each virus were prepared, and the plaque phenotypes of viruses in these stocks were compared with those of the original plaque isolates. No differences were seen; therefore, these nine *ts* mutant viruses could all be propagated at the permissive condition without phenotypic reversion. Figure 2

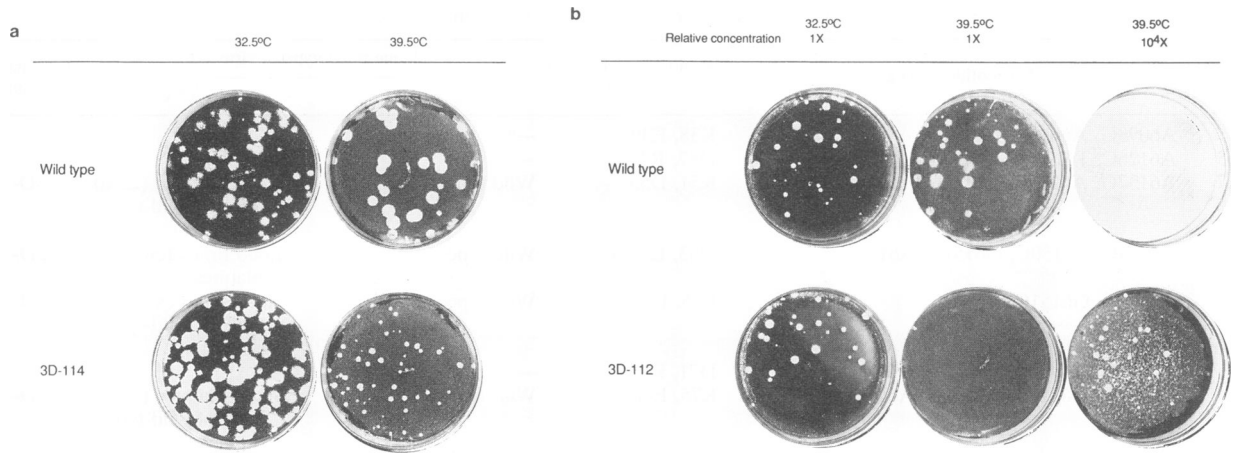

FIG. 2. Plaque phenotypes of wild-type poliovirus Mahoney type 1 and *ts* mutant viruses. (a) Wild type and *ts* small-plaque mutant 3D-114. (b) Wild type and *ts* plaque reduction mutant 3D-112. Infected monolayers were incubated either at 32.5°C for 72 h or at 39.5°C for 48 h.

shows the results of plaque assays of high-titer stocks of wild-type virus and two mutants, *ts* small-plaque mutant 3D-114 (Fig. 2a) and *ts* plaque reduction mutant 3D-112 (Fig. 2b). Other *ts* small-plaque mutants displayed a range of plaque sizes at 39.5°C, with 3D-108 showing the least dramatic, although still quite apparent, *ts* small-plaque phenotype (Table 1). In plaque assays of the three *ts* plaque reduction mutants, all behaved similarly to 3D-112 (Fig. 2b), forming approximately 1,000-fold fewer plaques at 39.5 than at 32.5°C (Table 1). Those plaques that did form after the plaque-reduction mutants 3D-107, 3D-112, and 3D-113 were plated at 39.5°C were heterogeneous in size. Several such plaques were isolated and found to harbor phenotypically revertant virus, with a much lower ratio of plaque formation at 32.5°C to that at 39.5°C than the original *ts* mutant virus (data not shown).

To determine whether the introduced clustered charged-to-alanine mutations were responsible for the mutant phenotypes of the *ts* viruses, the mutagenized region of each cDNA was sequenced. Depending on the location of the introduced mutations, different regions of the 3D coding region were present in the subclone that was subjected to site-directed mutagenesis. For *ts* viruses 3D-106 through 3D-113, the corresponding cDNAs were sequenced from nt 5601 to 7053; for *ts* virus 3D-114, the corresponding cDNA was sequenced from nt 7053 to the end of the poliovirus cDNA. Each of the nine cDNAs that gave rise to *ts* viruses contained the intended mutations (Table 1). One mutated cDNA, 3D-113, contained an additional, unplanned nucleotide change (A to G at nt 6777) predicted to cause an amino acid change (tyrosine to cystine at amino acid 264). Thus, in addition to the clustered charged-to-alanine mutations that were introduced, another amino acid substitution may contribute to the *ts* phenotype of 3D-113 virus. No other changes in the mutated poliovirus cDNAs were found.

To determine whether the introduced clustered charged-to-alanine mutations were present in the mutant viral RNAs recovered following transfection of mutant cDNAs, the presence of each mutation in viral RNA was verified by sequence analysis. For each of the nine stable *ts* mutants in Table 2, cDNA complementary to the region surrounding the introduced mutations was synthesized and subsequently amplified by PCR (35). When these PCR products, which should represent the viral RNA sequences from which the cDNA was made, were sequenced, no evidence of reversion of the introduced mutations was found.

Given the high error rates of RNA-dependent RNA polymerases in general (64, 65) and of the poliovirus polymerase in particular (75), the lack of additional mutations in the transfected poliovirus cDNAs and the lack of reversion at the site of the mutation in the resulting viral RNAs cannot ensure that the mutant viral RNAs obtained following transfection contained no additional mutations anywhere in the genome. It is always possible that the viruses that were selected, those that formed plaques after transfection of the cDNAs, arose from a minority of RNA species that contained additional mutations that increased their viability. Two lines of evidence argue against this possibility for any of the *ts* viruses in this study. First, the phenotypes of the five plaques selected from each cDNA transfection were identical; thus, if the viral genomes in these five plaques are not identical to the transfected cDNA, but instead contain mutations that allow phenotypic reversion, either identical mutations occurred and were selected multiple times or different suppressor mutations yielded viruses with identical phenotypes. In addition, the transfection efficiencies, that is, the number of plaques that arose at 32.5°C following transfection of comparable amounts of mutated and wild-type cDNA-containing plasmids, were comparable for the mutated and wild-type cDNAs (data not shown). Thus, if additional suppressing mutations occurred in the RNA, they were generated at a sufficiently high frequency that the number of plaques obtained from DNA transfection was not reduced. It is therefore extremely likely that the *ts* phenotypes of 3D-106, 3D-107, 3D-108, 3D-109, 3D-110, 3D-111, 3D-112, and 3D-114 were caused by the clustered charged-to-alanine mutations. For 3D-113, in which an additional, unintentional point mutation was found, it is not clear whether the intended set of mutations or the additional single-nucleotide substitution at nt 6777 (Table 1) was responsible for the *ts* phenotype. Since the 3D-113 virus was found to have defects in protein processing as well as in RNA synthesis (see below) and we are primarily interested in mutants with defects only in RNA synthesis, the intended and unintended mutations present in the cDNA that gave rise to *ts* virus 3D-113 were not introduced individually into full-length poliovirus cDNA clones to determine which was responsible for the *ts* phenotype.

Reduced accumulation of virus and RNA of *ts* mutants

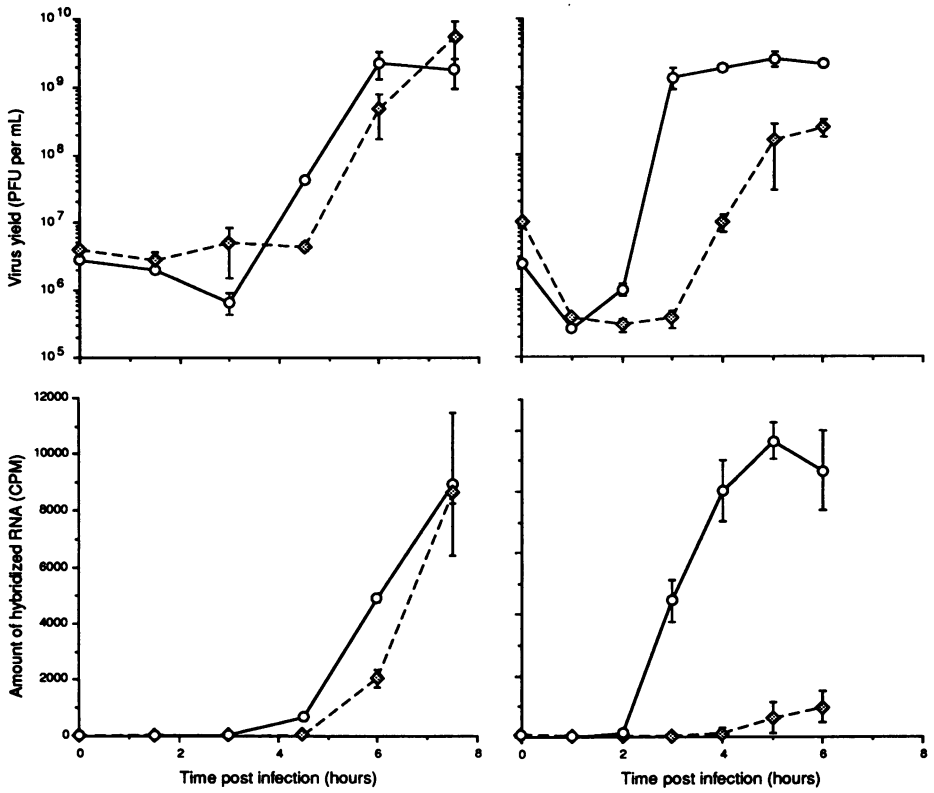

FIG. 3. Single-cycle infections showing accumulation of virus and positive-strand RNA for both wild-type and 3D-112 viruses. Constant-temperature infections were performed at 32.5°C, the permissive temperature (left panels), and at 39.5°C, the nonpermissive temperature (right panels), for the *ts* mutant virus. Virus yield was determined by plaque assay at 32.5°C, and accumulation of positive-strand RNA was measured by quantitative dot blot hybridization (35) as described in Materials and Methods. Solid lines depict wild-type virus; dashed lines depict mutant virus. Means ± standard deviations are shown.

during constant-temperature infections at 39.5°C. As a first step in characterizing the *ts* defects of the mutants, intracellular virus production and positive-sense viral RNA accumulation of wild-type and mutant viruses were measured during constant-temperature infections at both 32.5 and 39.5°C. HeLa suspension cultures were infected with wild-type and mutant viruses at MOIs of 50 and incubated at either 32.5 or 39.5°C. Samples were taken at intervals, and cytoplasmic extracts were prepared for analysis of virus production by plaque assay and for analysis of positive-strand RNA accumulation by quantitative dot blot hybridization. Figure 3 shows the results of a representative experiment performed with wild-type virus and *ts* mutant 3D-112. At 32.5°C, only slight differences in virus production and RNA accumulation between the mutant and the wild type were observed. At 39.5°C, however, both virus production and RNA accumulation were reduced at least 10-fold in infections with 3D-112 compared with those in wild-type infections.

Table 2 summarizes the results of these experiments for the nine stable *ts* mutants. Eight of the *ts* mutants showed temper-

TABLE 2. Summary of results of constant-temperature infections at permissive (32.5°C) and nonpermissive (39.5°C) temperature for *ts* viruses

Virus	Virus yield[a] at:		RNA accumulation[a] at:		*ts* defect(s)
	32.5°C	39.5°C	32.5°C	39.5°C	
3D-106	wt	wt	0.8 wt	0.6 wt	Slightly *ts* for RNA accumulation
3D-107	wt	0.1 wt	0.5 wt	0.1 wt	*ts* for virus yield and RNA accumulation
3D-108	1.4 wt	wt	0.5 wt	0.5 wt	
3D-109	wt	wt	0.6 wt	0.4 wt	Slightly *ts* for RNA accumulation
3D-110	0.6 wt	0.4 wt	1.5 wt	0.6 wt	Slightly *ts* for virus yield and *ts* for RNA accumulation
3D-111	0.6 wt	0.2 wt	0.4 wt	wt	*ts* for virus yield
3D-112	wt	0.1 wt	wt	0.1 wt	*ts* for virus yield and RNA accumulation
3D-113[b]	wt	0.1 wt	1.3 wt	0.2 wt	*ts* for virus yield and RNA accumulation
3D-114	0.8 wt	0.3 wt	wt	0.3 wt	*ts* for virus yield and RNA accumulation

[a] Maximum yield. wt, wild type.
[b] An additional nucleotide change, A6777G, resulted in amino acid substitution Y264C.

TABLE 3. Virus yield following RNA transfection under permissive (32.5°C) and nonpermissive (39.5°C) conditions for *ts* mutants 3D-107 and 3D-112

Virus	Replicate	Virus yield (PFU/ml) at:		Virus yield ratio (39.5°C/32.5°C)
		32.5°C	39.5°C	
Wild type	1	5,000	300,000	60
	2	10,000	600,000	60
	3	8,000	500,000	62
3D-107	1	2,000	60	0.03
	2	8,000	80	0.01
3D-112	1	200	10	0.05
	2	300	45	0.15

ature-dependent reductions of various degrees in virus yield or RNA accumulation at 39.5°C, the nonpermissive temperature. The severity of the reductions in virus and RNA accumulation correlated with the severity of the *ts* plaque phenotypes. 3D-108, which displayed the least severe plaque phenotype, displayed no *ts* defect in constant-temperature infections, while the three plaque reduction mutants, 3D-107, 3D-112, and 3D-113, showed the most severe *ts* defects in constant-temperature infections. 3D-111 displayed a *ts* defect only in virus yield. Several possibilities could explain this: 3D-111 might have no *ts* defect in RNA accumulation, it might have too subtle a defect to be distinguished by this assay, or a defect might be masked by feedback from other processes during a single cycle. These possibilities were further tested by temperature shift experiments.

Two *ts* mutants, 3D-107 and 3D-112, displayed an additional defect in cell entry that resulted in a delay in progression through the infectious cycle that was apparent at both temperatures in these constant-temperature, single-cycle infections (unpublished results). In the present study, however, we consider the *ts* phenotypes of 3D-107 and 3D-112 independently of their slow-eclipse phenotypes. This is justified because the temperature sensitivity of 3D-107 and 3D-112 virus production was still observed when normal cell entry steps were bypassed by initiating wild-type, 3D-107, and 3D-112 infections with RNA transcripts (Table 3).

Temperature shift experiments to monitor translation, protein processing, and protein stability of *ts* mutant viruses. Most of the nine stable *ts* mutants displayed reduced accumulation of positive-strand RNA during single-cycle infections at 39.5°C, the temperature at which they also formed smaller or fewer plaques than wild-type viruses. However, *ts* defects in cell entry, translation of the viral genome, processing of viral polypeptides, or stability of the viral polypeptides, by reducing the intracellular concentrations of viral proteins, could reduce the rate of RNA replication and result in an apparent RNA accumulation defect in constant-temperature experiments. Such defects might also account for the plaque phenotypes of those mutants that showed no reduction in virus or RNA accumulation in constant-temperature infections. It is also possible that defects in RNA accumulation could be masked by feedback from these processes during long periods of infection. Thus, we tested whether any of the *ts* mutants showed *ts* defects in translation, protein processing, protein stability, or RNA synthesis after temperature shift, to try to study the temperature sensitivity of each of these processes in isolation.

To assess the effect of temperature shift on translation, the accumulation of labeled viral proteins after a shift from the permissive to the nonpermissive temperature was monitored. HeLa monolayers were infected with wild-type or mutant viruses and incubated for 7 h at 32.5°C, the permissive condition; at this stage of infection, translation of the majority of host cell proteins should be inhibited, and newly synthesized proteins should be almost exclusively viral (63). At 7 h postinfection, [^{35}S]methionine was added and the incubations were either continued at 32.5°C or shifted to 39.5°C. Following 15 min of incubation, cytoplasmic extracts were prepared and the amount of trichloroacetic acid-precipitable radioactivity was determined. As shown in Table 4, none of the *ts* mutants exhibited a *ts* reduction in the accumulation of labeled viral proteins. In fact, several mutants showed significant increases in viral protein accumulation at 39.5°C after the temperature shift compared with that of the wild type. We have, at present, no explanation for this observation; it is possible that reduced rates of RNA synthesis (see below) can lead to greater utilization of viral positive strands as mRNAs. SDS-PAGE analysis (Fig. 4) of all of the extracts demonstrated that, for each mutant, inhibition of host translation occurred by 7 h postinfection at 32.5°C and that the yield and distribution of viral polypeptides synthesized at 39.5°C were equivalent to those observed in wild-type infections. Thus, none of these mutants displayed a *ts* defect in translation.

To assess the effect of temperature shift on the processing and stability of viral proteins, HeLa cell monolayers were again infected with wild-type or mutant virus and incubated for 7 h at 32.5°C. However, in these experiments, labeling with [^{35}S]methionine was performed for 15 min at 32.5°C immediately before the temperature shifts. Medium containing excess un-

TABLE 4. Summary of temperature shift experiments for *ts* mutants

Virus	Translation (cpm, 39.5/32.5°C)	RNA accumulation (cpm, 39.5/32.5°C)	*ts* defect
Wild type	1.1 ± 0.2	2.9 ± 0.8	
3D-106	2.0 ± 0.4	1.2 ± 0.3	*ts* for RNA accumulation
3D-107	1.0 ± 0.1	0.7 ± 0.1	*ts* for RNA accumulation
3D-108	1.4 ± 0.2	1.4 ± 0.2	*ts* for RNA accumulation
3D-109	1.3 ± 0.2	5.2 ± 1.2	
3D-110	1.6 ± 0.1	0.9 ± 0.2	*ts* for RNA accumulation
3D-111	2.0 ± 0.1	1.3 ± 0.3	*ts* for RNA accumulation
3D-112	1.0 ± 0.2	1.1 ± 0.4	*ts* for RNA accumulation
3D-113[a]	1.3 ± 0.4	Not tested	
3D-114	1.1 ± 0.2	1.5 ± 0.6	*ts* for RNA accumulation[b]

[a] An additional nucleotide change, A6777G, resulted in amino acid substitution Y264C.
[b] Different from wild type with greater than 90% confidence by Student's *t* test.

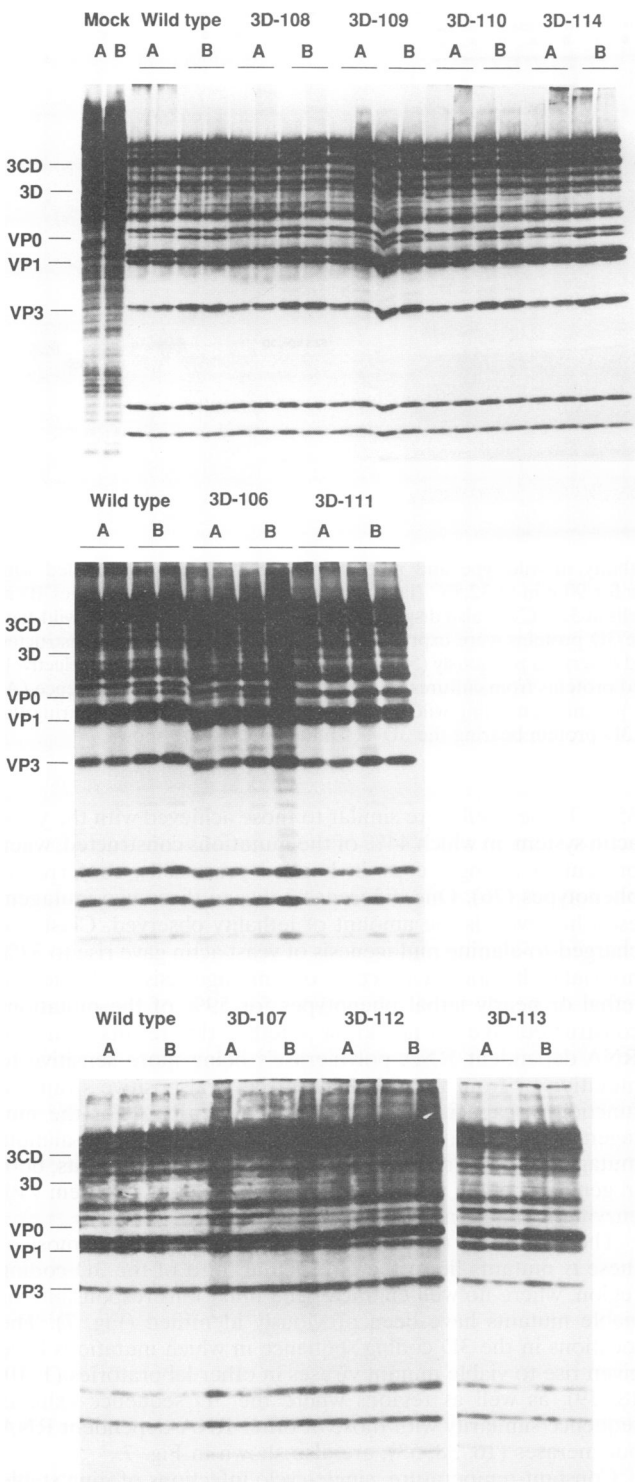

FIG. 4. Effect of temperature shift on accumulation of newly synthesized proteins in wild-type and *ts* mutant-infected cells at permissive and nonpermissive temperatures. The amount of trichloroacetic acid-precipitable radioactivity was determined by labeling cells infected with wild-type or mutant viruses 7 h postinfection at 32.5°C with [^{35}S]methionine for 15 min at either 32.5°C (lanes A) or 39.5°C (lanes B) as described in Materials and Methods. The viral proteins are identified at left; they were identified by comparing the mobilities of the labeled viral proteins with those of unlabeled protein markers and labeled capsid proteins electrophoresed on the same gels and by comparison with similar gels from other laboratories (6, 19). Labeled proteins from mock-infected cells at 32.5 and 39.5°C are also displayed.

labeled methionine was then added to identical cultures, which were then incubated either for 90 min at 32.5°C or for 60 min at 39.5°C to chase the labeled polypeptides under permissive and nonpermissive conditions. Cytoplasmic extracts were prepared and analyzed by SDS-PAGE (Fig. 5a). Mutants 3D-107, -108, -109, -112, and -114 revealed no defects in protein processing: no novel bands or altered polypeptide mobilities were observed with or without the temperature shift. The slight differences in the extents of protein processing between infections were not temperature dependent.

For four of the *ts* mutants, alterations in the mobilities of viral polypeptides were observed. Three mutants, 3D-106, 3D-110, and 3D-111, showed altered mobilities of all polypeptides containing the N-terminal sequences of 3D, where the mutations responsible for the mutant phenotypes mapped (Fig. 1 and Table 1). For each of these mutants, bands corresponding to 3D, 3CD, and 3C′ displayed greater electrophoretic mobilities than their wild-type counterparts (Fig. 5a). To determine whether these mobility shifts resulted from altered electrophoretic mobility of the mutant proteins or altered sites of protein processing, the 3D coding regions from 3D-106, 3D-110, and 3D-111 were expressed in *E. coli*. As shown in Fig. 5b, the observed mobilities of mutant and wild-type 3D were identical in virus-infected and bacterial cells. Furthermore, sequence analysis excluded the possibility that small deletions had been introduced into the 3D coding sequences. Therefore, the mobility shifts of 3D N-terminus-containing polypeptides of mutants 3D-106, 3D-110, and 3D-111 were not due to defects in protein processing but are intrinsic to the mutant polypeptides, possibly reflecting altered extents of SDS binding.

Another *ts* mutant, 3D-113, displayed a novel band below that of capsid polypeptide VP1 at both temperatures (Fig. 5a). Although the origin of this band has not yet been determined, it is clear that 3D-113 mutant viruses, unlike the other *ts* mutants, displayed a defect in protein processing that may or may not be responsible for the decreased accumulation of viral RNA observed in constant-temperature infections.

ts mutations often affect the folding of mutant proteins (2), which can result in increased susceptibility of mutant proteins to intracellular proteases. Comparison of the intensities of the viral protein bands in Fig. 5a, labeled at the permissive temperature and subsequently incubated at the permissive and nonpermissive temperatures, reveals no significant change in the half-life of mutant 3D-containing polypeptides at the nonpermissive temperature.

ts mutants 3D-106, 3D-107, 3D-108, 3D-109, 3D-110, 3D-111, 3D-112, and 3D-114 thus display no defects in translation, protein processing, or protein stability that can explain their *ts* phenotypes. Each of these mutants was studied further to determine whether it displayed a primary defect in RNA synthesis as assayed by temperature shift. 3D-113, on the other hand, displayed a defect in protein processing, accumulating a novel polypeptide at both the permissive and nonpermissive temperatures. Therefore, it would be difficult to establish a primary defect in RNA synthesis for this mutant, and 3D-113 was not studied further.

Temperature shift experiments to monitor accumulation of positive-strand RNA. To determine whether any of the *ts* mutants has a primary defect in RNA replication, we again

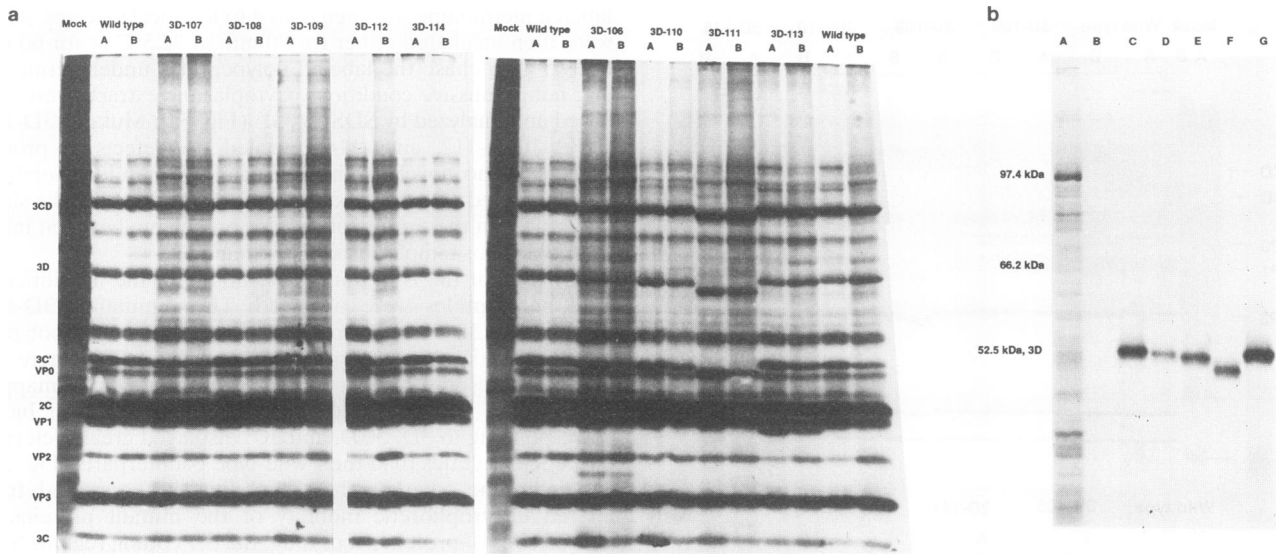

FIG. 5. (a) Effect of temperature shift on protein processing and stability in wild-type and mutant infections. Cells were labeled with [^{35}S]methionine for 15 min at 6 h postinfection at 32.5°C and chased either for 90 min at 32.5°C (lanes A) or for 60 min at 39.5°C (lanes B) as described in Materials and Methods. Labeled proteins from mock-infected cells at 32.5°C are also displayed. (b) SDS-PAGE mobilities of wild-type and selected 3D mutant proteins expressed in *E. coli*. Mutant and wild-type 3D proteins were expressed from a plasmid, pT5T-3D, constructed by T. Jarvis (Ribozyme Products, Inc.) and similar to a 3D-expression plasmid described previously (52). Plasmid-encoded proteins were selectively labeled with [^{35}S]methionine as described in Materials and Methods. Labeled proteins from cultures of *E. coli* with no plasmid in the absence (A) and presence (B) of rifampin and from rifampin-treated *E. coli* containing plasmids encoding wild-type 3D (C and G), 3D protein bearing the 3D-106 mutations (D), 3D protein bearing the 3D-110 mutations (E), and 3D protein bearing the 3D-111 mutations (F) are shown.

performed temperature shift experiments in which viral proteins and RNA were allowed to accumulate at the permissive temperature. Then, at 4 h postinfection at 32.5°C, incubations of duplicate cultures were continued at either 32.5 or 39.5°C, samples were taken at intervals, and cytoplasmic extracts were prepared for analysis of RNA accumulation by quantitative dot blot hybridization. The temperature was shifted at an earlier time in the infectious cycle than in the previous temperature shift experiments because of the decreased sensitivity of assays to detect the new synthesis of RNA compared with assays to detect the new synthesis of viral polypeptides. Figure 6a shows that in infections with wild-type poliovirus, more RNA accumulated when the temperature was shifted to 39.5°C than when the incubation was continued at 32.5°C. In infections with *ts* mutant 3D-107 (Fig. 6b), however, less RNA accumulated after the shift to 39.5°C than when the incubations were continued at the permissive temperature. These data for the 6-h time points of wild-type and 3D-107 infections, as well as for temperature-shifted infections with 3D-106, 3D-109, 3D-110, 3D-111, 3D-112, 3D-113, and 3D-114, are shown in Fig. 6c. Each mutant, with the exception of 3D-109, showed a significant decrease in RNA accumulation at the nonpermissive condition relative to that of wild-type poliovirus.

DISCUSSION

Using a clustered charged-to-alanine mutagenesis strategy, in which clusters of codons for charged amino acids are replaced by alanine codons, an array of *ts* alleles of the 3D coding region was generated. Thirty-seven percent of the mutant cDNAs constructed gave rise to mutant viruses with *ts* phenotypes. However, one of these cDNAs contained an additional single-nucleotide substitution (Tables 1 and 2), thus reducing the yield of *ts* mutants whose phenotypes are known to be caused by the clustered charged-to-alanine mutations to 35%. These results are similar to those achieved with the yeast actin system, in which 44% of the mutations constructed, when present in a single copy in haploid yeast cells, conferred *ts* phenotypes (76). One difference between these two mutageneses, however, is the amount of lethality observed. Clustered charged-to-alanine mutagenesis of yeast actin gave rise to 32% nonviable haploid yeast cells; our mutagenesis of 3D led to lethal or nearly lethal phenotypes for 59% of the mutations constructed. We do not know whether this results from the RNA-dependent RNA polymerase's being more sensitive to mutation or from the necessity of the viral positive strand to function in capacities other than as the mRNA for the mutagenized protein. In any case, clustered charged-to-alanine mutagenesis gave rise to a high percentage of *ts* mutants, both in genes encoding a structural protein (76) and a protein with enzymatic function.

The mutations responsible for the phenotypes of most of these *ts* mutants lie in the N-terminal third of the 3D coding region, where no well-characterized mutations responsible for viable mutants have been previously identified (Fig. 7). The locations in the 3D coding sequence in which mutations have given rise to viable mutant viruses in other laboratories (1, 10, 18, 19), as well as regions where the 3D sequence exhibits sequence similarity with those of other RNA-dependent RNA polymerases (16, 38, 53), are also shown in Fig. 7.

Constant-temperature, single-cycle infections of nine stable *ts* mutants displayed defects in viral yield or RNA accumulation for eight of the mutants, with the severity of defects mirrored by the severity of plaque defects (Tables 1 and 2). For example, mutant 3D-108, which displayed no defects in viral yield or in RNA accumulation in single-cycle infections, also displayed the least severe small-plaque phenotype, whereas the plaque reduction mutants 3D-107, 3D-112, and 3D-113 all displayed severe defects in both viral yield and RNA accumulation.

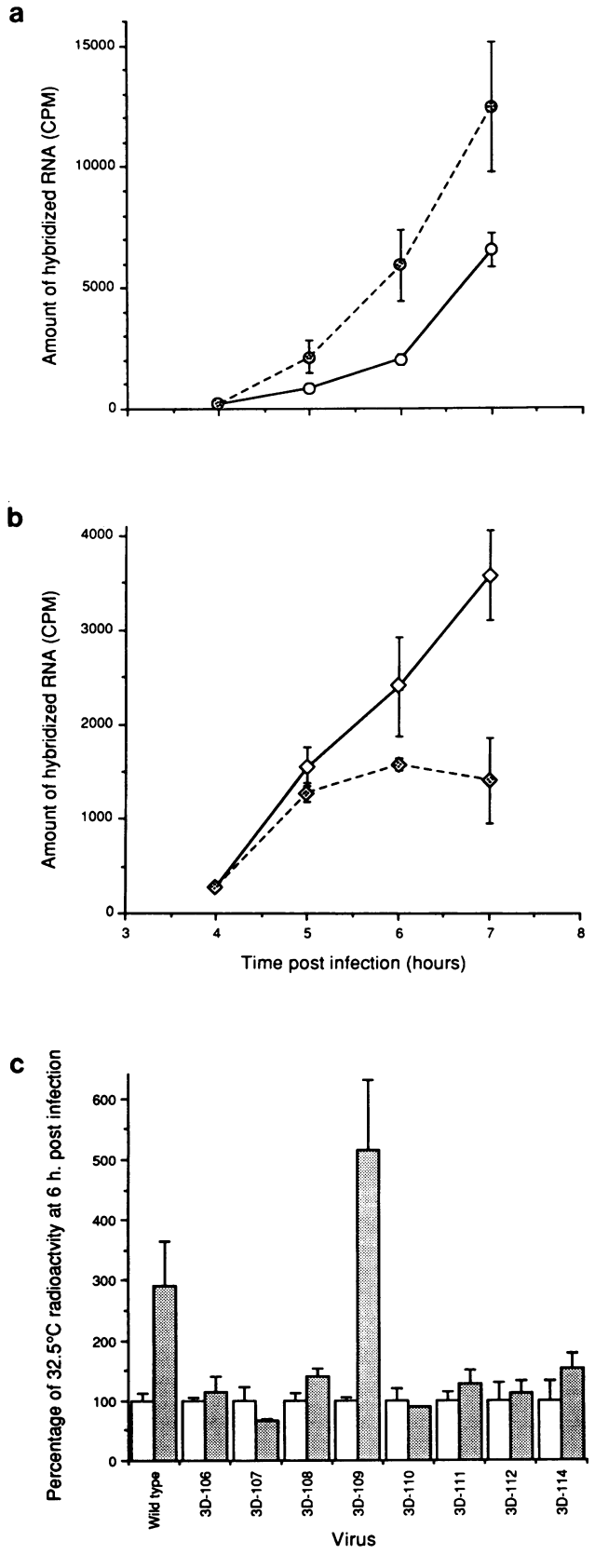

Temperature shift experiments allowed us to identify the first step in viral replication after cell entry in which each mutant displayed a biochemical defect. None of the *ts* mutant viruses displayed any defects in translation or in protein stability compared with wild-type virus. One of the *ts* mutant viruses, 3D-113, displayed a defect in the processing of viral polypeptides. The remaining eight *ts* mutant viruses, however, showed no defects in viral protein processing.

It was during the analysis of positive-strand RNA accumulation that most of the *ts* mutant viruses displayed defects dependent on a temperature shift. Mutants 3D-106, 3D-107, 3D-108, 3D-110, 3D-111, 3D-112, and 3D-114 all exhibited a decrease in RNA accumulation compared with that in wild-type virus 2 h after a shift to the nonpermissive temperature. 3D-113 was not tested in these experiments because its defect in protein processing would make it difficult to interpret any temperature-dependent effect on RNA accumulation. Of the viruses tested, only 3D-109 showed no temperature-dependent defect in RNA accumulation. We do not know whether the failure to display a defect in RNA accumulation after the temperature shift resulted from the subtlety of the mutant phenotype or from a defect elsewhere in the viral replicative cycle, for example, in establishing but not maintaining the replication complex (48).

Each set of mutations introduced created changes in both the positive- and negative-strand viral RNAs as well as in the amino acid sequences of 3D and related polypeptides. For simplicity, the mutants resulting from clustered charged-to-alanine scanning mutagenesis have been discussed as though the relevant changes were in the amino acid sequence. However, *ts* mutants of poliovirus with defects in RNA accumulation have been described previously whose only mutations were in the 3′ noncoding region (61) or the 5′ noncoding region (3, 24, 57). Furthermore, it is possible that *cis*-dominant poliovirus mutants bearing mutations in the coding regions of 2B (46), 3A (27), and 3D (10) owe their mutant phenotypes to defects in RNA structure or sequence. Experiments to test the recessive, *cis*-dominant, or dominant nature of these mutant phenotypes have not been performed; however, by analogy with the *S. cerevisiae ACT1* mutants (76), it is likely that the defects caused by each of these sets of mutations are due, at least in part, to the mutations in the protein sequence.

Seven of the *ts* mutants generated in this study, 3D-106, 3D-107, 3D-108, 3D-110, 3D-111, 3D-112, and 3D-114, displayed *ts* plaque phenotypes that correlated with *ts* defects in RNA accumulation after temperature shift. The mutations responsible for the *ts* phenotype of 3D-114 lie near the C

FIG. 6. Effect of temperature shift on accumulation of positive-strand RNA in infections with wild-type and *ts* mutant polioviruses. Means and standard deviations are shown. (a) HeLa cells were infected with wild-type poliovirus at 32.5°C. At 4 h postinfection, the incubations were continued at either 32.5°C (solid line) or 39.5°C (dashed lines), and the subsequent accumulation of positive-strand RNA was monitored by dot blot hybridization. (b) Accumulation of positive-strand RNA in infections with *ts* mutant virus 3D-107 during continuous incubation at 32.5°C (solid line) and following a temperature shift to 39.5°C (dashed line) at 4 h postinfection. (c) Graphic representation of the relative accumulation of positive-strand RNA in wild-type and *ts* mutant-infected cells with and without temperature shift. For each virus, the accumulation of RNA at 6 h postinfection, following continuous incubation at 32.5°C, was normalized to 100% (open bars). The shaded bars show the relative amounts of positive-strand RNA that accumulated by the 6-h time point when the temperature was shifted to 39.5°C at 4 h postinfection.

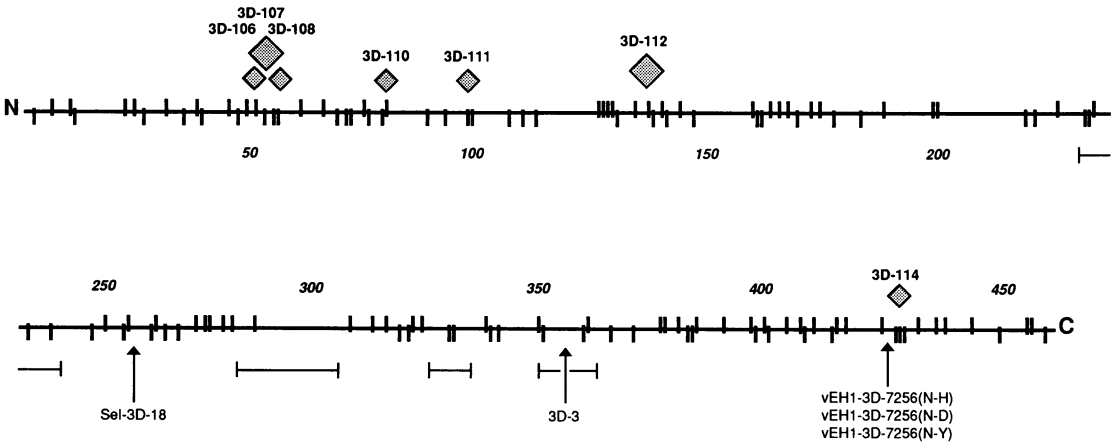

FIG. 7. Schematic representation of the 461-amino-acid sequence of 3D, the poliovirus RNA-dependent RNA polymerase, showing the locations of charged residues and clustered charged-to-alanine mutations. The locations of acidic residues are shown by short vertical slashes below the horizontal line that represents the 461-amino-acid sequence; basic residues are shown by slashes above the line. The locations of the mutations in 3D-106, 3D-107, 3D-108, 3D-110, 3D-111, 3D-112, and 3D-114, those *ts* mutants that displayed specific defects in RNA accumulation in temperature shift experiments, are shown as follows: ◇, *ts* virus with a plaque reduction phenotype; ◇, *ts* virus with a small-plaque phenotype. Regions of homology with other RNA-dependent RNA polymerases (16, 38, 53) are depicted by brackets. Region A, amino acids 225 to 240; region B, amino acids 279 to 305; region C: amino acids 323 to 333; region D, amino acids 349 to 361. The locations of mutations that have been previously demonstrated to give rise to viable viruses with conditionally defective mutant phenotypes are indicated by arrows (1, 10, 18, 19).

terminus of the 3D protein (Fig. 7), only two amino acids away from Asn-424; mutations in Asn-424 are responsible for the *ts* phenotypes of three mutants studied previously (1, 18). One of these mutants, vEH1-3D-7256(N-H), showed a lower ratio of positive to negative strands in constant-temperature infections performed at high temperature than in those at low temperature, suggesting a specific defect in positive-strand synthesis at the nonpermissive temperature (18). It will be interesting to test whether 3D-114 displays a specific defect in positive-strand synthesis in temperature shift experiments. The mutations responsible for the *ts* phenotypes of 3D-106, 3D-107, 3D-108, 3D-110, 3D-111, and 3D-112 all lie in the N-terminal third of the 3D coding region (Fig. 7). No viable mutants with mutations in this region of 3D have been identified previously, and this region displays no sequence similarity with other RNA-dependent RNA polymerases (16, 38, 53).

The most severe biochemical and plaque morphology phenotypes were exhibited by *ts* mutants 3D-107, 3D-112, and 3D-114. These mutants are quite suitable for genetic studies that require pronounced plaque phenotypes. For yeast actin, it was shown that clustered charged-to-alanine mutagenesis specifically targeted patches of charged residues on the protein surface (76). For tissue plasminogen activator, 90% of the mutant proteins that resulted from a similar mutagenesis protocol were stable and properly folded when expressed in bacteria (8). As discussed in the introduction, it is possible that the reason this mutagenesis algorithm can generate *ts* mutants at such a high frequency in actin, and in the 3D polymerase, is that the targeted clusters of surface charges are normally involved in hydrogen bonding or electrostatic interactions with water or other proteins (2) and that these interactions are crucial for protein folding, function, or both. If this is the case, suppression analysis of mutant alleles generated by clustered charged-to-alanine mutagenesis may prove especially fruitful to identify proteins that interact functionally with the wild-type proteins (76). In the case of 3D, suppression analysis (3, 4, 24, 34, 47) of these alleles may identify other components of the poliovirus replication complex that interact functionally with the RNA-dependent RNA polymerase during the poliovirus infectious cycle.

ACKNOWLEDGMENTS

We thank Peter Sarnow, Mary T. L. Beckman, and Janice A. Pata for helpful comments on the manuscript and David Botstein for communication of results prior to publication. S.E.D. thanks Ben Young for advice on constructing mutant cDNAs.

This research was supported by NIH grant AI-25166 and by the David and Lucile Packard Foundation. S.E.D. was supported by fellowships from the NSF and the Colorado Institute for Research in Biotechnology. We are grateful to the Keck Foundation for generous support of RNA research in Boulder. K.K. is an assistant investigator of the Howard Hughes Medical Institute.

REFERENCES

1. **Agut, H., K. M. Kean, O. Fichot, J. Morasco, J. B. Flanegan, and M. Girard.** 1989. A point mutation in the poliovirus polymerase gene determines a complementable temperature-sensitive defect of RNA replication. Virology **168:**302–311.
2. **Alber, T.** 1989. Mutational effects on protein stability. Annu. Rev. Biochem. **58:**765–798.
3. **Andino, R., G. E. Rieckhof, and D. Baltimore.** 1990. A functional ribonucleoprotein complex forms around the 5′ end of poliovirus RNA. Cell **63:**369–380.
4. **Andino, R., G. E. Rieckhof, D. Trono, and D. Baltimore.** 1990. Substitutions in the protease 3C gene of poliovirus can suppress a mutation in the 5′ noncoding region. J. Virol. **64:**607–612.
5. **Argos, P.** 1988. A sequence motif in many polymerases. Nucleic Acids Res. **16:**9909–9916.
6. **Barton, D. J., and J. B. Flanegan.** 1993. Coupled translation and replication of poliovirus RNA in vitro: synthesis of functional 3D polymerase and infectious virus. J. Virol. **67:**822–831.
7. **Bass, S. H., M. G. Mulkerrin, and J. A. Wells.** 1991. A systematic mutational analysis of hormone-binding determinants in the human growth hormone receptor. Proc. Natl. Acad. Sci. USA **88:**4498–4502.
8. **Bennett, W. F., N. F. Paoni, B. A. Keyt, D. Botstein, J. J. S. Jones, L. Presta, F. M. Wurm, and M. J. Zoller.** 1991. High resolution analysis of functional determinants on human tissue-type plasminogen activator. J. Biol. Chem. **266:**5191–5201.

9. **Bernstein, H. D., and D. Baltimore.** 1988. Poliovirus mutant that contains a cold-sensitive defect in viral RNA synthesis. J. Virol. **62:**2922–2928.
10. **Bernstein, H. D., P. Sarnow, and D. Baltimore.** 1986. Genetic complementation among poliovirus mutants derived from an infectious cDNA clone. J. Virol. **60:**1040–1049.
11. **Bienz, K., D. Egger, T. Pfjister, and M. Troxler.** 1992. Structural and functional characterization of the poliovirus replication complex. J. Virol. **66:**2740–2747.
12. **Bienz, K., D. Egger, Y. Rasser, and W. Bossart.** 1980. Kinetics and location of poliovirus macromolecular synthesis in correlation to virus-induced cytopathology. Virology **100:**390–399.
13. **Bienz, K., D. Egger, M. Troxler, and L. Pasamontes.** 1990. Structural organization of poliovirus RNA replication is mediated by viral proteins of the P2 genomic region. J. Virol. **64:**1156–1163.
14. **Blair, W. S., and B. L. Semler.** 1991. Role for the P4 amino acid residue in substrate utilization by the poliovirus 3CD proteinase. J. Virol. **65:**6111–6123.
15. **Blumenthal, T., T. A. Landers, and K. Wever.** 1972. Bacteriophage Qβ replicase contains the protein biosynthesis elongation factors EF Tu and EF Ts. Proc. Natl. Acad. Sci. USA **69:**1313–1317.
16. **Bruenn, J. A.** 1991. Relationships among the positive strand and double-strand RNA viruses as viewed through their RNA-dependent RNA polymerases. Nucleic Acids Res. **19:**217–226.
17. **Burns, C. C., M. A. Lawson, B. L. Semler, and E. Ehrenfeld.** 1989. Effects of mutations in poliovirus 3Dpol on RNA polymerase activity and on polyprotein cleavage. J. Virol. **63:**4866–4874.
18. **Burns, C. C., O. C. Richards, and E. Ehrenfeld.** 1992. Temperature-sensitive polioviruses containing mutations in RNA polymerase. Virology **189:**568–582.
19. **Charini, W. A., C. C. Burns, E. Ehrenfeld, and B. L. Semler.** 1991. *trans* rescue of a mutant poliovirus RNA polymerase function. J. Virol. **65:**2655–2665.
20. **Cunningham, B. C., and J. A. Wells.** 1989. High-resolution epitope mapping of hGH-receptor interactions by alanine-scanning mutagenesis. Science **244:**1081–1085.
21. **Dao-pin, S., D. E. Anderson, W. A. Baase, F. W. Dahlquist, and B. W. Matthews.** 1991. Structural and thermodynamic consequences of burying a charged residue within the hydrophobic core of T4 lysozyme. Biochemistry **30:**11521–11529.
22. **Dasgupta, A., M. H. Baron, and D. Baltimore.** 1979. Poliovirus replicase: a soluble enzyme able to initiate copying of poliovirus RNA. Proc. Natl. Acad. Sci. USA **76:**2679–2683.
23. **Delarue, M., O. Poch, N. Tordo, D. Moras, and P. Argos.** 1990. An attempt to unify the structure of polymerases. Protein Eng. **3:**461–467.
24. **Dildine, S. L., and B. L. Semler.** 1989. The deletion of 41 proximal nucleotides reverts a poliovirus mutant containing a temperature-sensitive lesion in the 5′ noncoding region of genomic RNA. J. Virol. **63:**847–862.
25. **Dorssers, L., S. van der Krol, J. van der Meer, A. van Kammen, and P. Zabel.** 1984. Purification of cowpea mosaic virus RNA replication complex: identification of a virus-encoded 110,000-dalton polypeptide responsible for RNA chain elongation. Proc. Natl. Acad. Sci. USA **81:**1951–1955.
26. **Fujimura, T., and R. B. Wickner.** 1989. Reconstitution of template-dependent in vitro transcriptase activity of a yeast double-stranded RNA virus. J. Biol. Chem. **264:**10872–10877.
27. **Giachetti, C., S. S. Hwang, and B. L. Semler.** 1992. *cis*-acting lesions targeted to the hydrophobic domain of a poliovirus membrane protein involved in RNA replication. J. Virol. **66:**6045–6057.
28. **Giachetti, C., and B. L. Semler.** 1991. Role of a viral membrane polypeptide in strand-specific initiation of poliovirus RNA synthesis. J. Virol. **65:**2647–2654.
29. **Gibbs, C. S., and M. J. Zoller.** 1991. Rational scanning mutagenesis of a protein kinase identifies functional regions involved in catalysis and substrate interactions. J. Biol. Chem. **266:**8923–8931.
30. **Grakoui, A., R. Levis, R. Raju, H. V. Huang, and C. Rice.** 1989. A *cis*-acting mutation in the Sindbis virus junction region which affects subgenomic RNA synthesis. J. Virol. **63:**5216–5227.
31. **Hayes, R. J., and K. W. Buck.** 1990. Complete replication of a eukaryotic virus RNA in vitro by a purified RNA-dependent RNA polymerase. Cell **63:**363–368.
32. **Jablonski, S. A., M. Luo, and C. D. Morrow.** 1991. Enzymatic activity of poliovirus RNA polymerase mutants with single amino acid changes in the conserved YGDD amino acid motif. J. Virol. **65:**4565–4572.
33. **Jablonski, S. A., and C. D. Morrow.** 1993. Enzymatic activity of poliovirus RNA polymerases with mutations at the tyrosine residue of the conserved YGDD motif: isolation and characterization of polioviruses containing RNA polymerases with FGDD and MGDD sequences. J. Virol. **67:**373–381.
34. **Jacobson, S. J., D. A. M. Konings, and P. Sarnow.** 1993. Biochemical and genetic evidence for a pseudoknot structure at the 3′ terminus of the poliovirus RNA genome and its role in viral RNA amplification. J. Virol. **67:**2961–2971.
35. **Jarvis, T., and K. Kirkegaard.** 1992. Poliovirus RNA recombination: mechanistic studies in the absence of selection. EMBO J. **11:**3135–3145.
36. **Johnson, K., and P. Sarnow.** 1991. Three poliovirus 2B mutants exhibit noncomplementable defects in viral RNA amplification and display dosage-dependent dominance over wild-type poliovirus. J. Virol. **65:**4341–4349.
37. **Jore, J., B. De Gues, R. J. Jackson, P. H. Pouwels, and B. E. Enger-Valk.** 1988. Poliovirus protein 3CD is the active protease for processing of the precursor protein *in vitro*. J. Gen. Virol. **69:**1627–1636.
38. **Kamer, G., and P. Argos.** 1984. Primary structural comparison of RNA-dependent polymerases from plant, animal and bacterial viruses. Nucleic Acids. Res. **12:**7269–7282.
39. **Kanaya, S., N. C. Katsuda, and M. Ikehara.** 1991. Importance of the positive charge cluster in Escherichia coli ribonuclease HI for the effective binding of the substrate. J. Biol. Chem. **266:**11621–11627.
40. **Kirkegaard, K., and D. Baltimore.** 1986. The mechanism of RNA recombination in poliovirus. Cell **47:**433–443.
41. **Kirkegaard, K., and B. Nelsen.** 1990. Conditional poliovirus mutants made by random deletion mutagenesis of infectious cDNA. J. Virol. **64:**185–194.
42. **Kitamura, N., B. Semler, P. Rothberg, G. Larsen, C. Adler, A. Dorner, E. Emini, R. Hanecak, J. Lee, S. van der Werf, C. Anderson, and E. Wimmer.** 1981. Primary structure, gene organisation, and polypeptide expression of poliovirus RNA. Nature (London) **291:**547–553.
43. **Kunkel, T. A.** 1985. Rapid and efficient site-specific mutagenesis without phenotypic selection. Proc. Natl. Acad. Sci. USA **82:**488–492.
44. **Laemmli, U. K.** 1970. Cleavage of structural proteins during the assembly of the head of bacteriophage T4. Nature (London) **227:**680–685.
45. **La Monica, N., C. Meriam, and V. R. Racaniello.** 1986. Mapping of sequences required for mouse neurovirulence of poliovirus type 2 Lansing. J. Virol. **57:**515–525.
46. **Li, J.-P., and D. Baltimore.** 1988. Isolation of poliovirus 2C mutants defective in viral RNA synthesis. J. Virol. **62:**4016–4021.
47. **Li, J.-P., and D. Baltimore.** 1990. An intragenic revertant of a poliovirus 2C mutant has an uncoating defect. J. Virol. **64:**1102–1107.
48. **Maynell, L. A., K. Kirkegaard, and M. W. Klymkowsky.** 1992. Inhibition of poliovirus RNA synthesis by brefeldin A. J. Virol. **66:**1985–1994.
49. **Mills, D. R., C. Priano, P. DiMauro, and B. D. Binderow.** 1988. Qβ replicase: mapping the functional domains of an RNA-dependent RNA polymerase. J. Mol. Biol. **205:**751–764.

49a. **Molla, A., A. Paul, and E. Wimmer.** Personal communication.

50. **Molla, A., A. V. Paul, and E. Wimmer.** 1991. Cell-free, de novo synthesis of poliovirus. Science **254:**1647–1651.
51. **Morrow, C. D., B. Warren, and M. R. Lentz.** 1987. Expression of enzymatically active poliovirus RNA-dependent RNA polymerase in Escherichia coli. Proc. Natl. Acad. Sci. USA **84:**6050–6054.
52. **Plotch, S. J., O. Palant, and Y. Gluzman.** 1989. Purification and properties of poliovirus RNA polymerase expressed in *Escherichia coli*. J. Virol. **63:**216–225.
53. **Poch, O., I. Sauvaget, M. Delarue, and N. Tordo.** 1989. Identification of four conserved motifs among the RNA-dependent polymerase encoding elements. EMBO J. **8:**3867–3874.

54. **Quadt, R., C. Koa, K. Borwinging, R. Hershberger, and P. Ahlquist.** 1993. Characterization of a host protein associated with brome mosaic virus RNA-dependent RNA polymerase. Proc. Natl. Acad. Sci. USA **90:**1498–1502.
55. **Racaniello, V. R., and D. Baltimore.** 1981. Cloned poliovirus complementary DNA is infectious in mammalian cells. Science **214:**916–919.
56. **Racaniello, V. R., and D. Baltimore.** 1981. Molecular cloning of poliovirus cDNA and determination of the complete nucleotide sequence of the viral genome. Proc. Natl. Acad. Sci. USA **78:**4887–4891.
57. **Racaniello, V. R., and C. Meriam.** 1986. Poliovirus temperature-sensitive mutant containing a single nucleotide deletion in the 5′ noncoding region of the viral RNA. Virology **155:**498–507.
58. **Ribas, J. C., and R. B. Wickner.** 1992. RNA-dependent RNA polymerase consensus sequence of the L-A double-stranded RNA virus: definition of essential domains. Proc. Natl. Acad. Sci. USA **89:**2185–2189.
59. **Sankar, S., and A. G. Porter.** 1992. Point mutations which drastically affect the polymerization activity of encephalomyocarditis virus RNA-dependent RNA polymerase correspond to the active site of *Escherichia coli* DNA polymerase. J. Biol. Chem. **267:** 10168–10176.
60. **Sarnow, P.** 1989. Role of 3′-end sequences in infectivity of poliovirus transcripts made in vitro. J. Virol. **63:**467–470.
61. **Sarnow, P., H. D. Bernstein, and D. Baltimore.** 1986. A poliovirus temperature-sensitive RNA synthesis mutant located in a noncoding region of the genome. Proc. Natl. Acad. Sci. USA **83:**571–575.
62. **Semler, B. L., R. J. Kuhn, and E. Wimmer.** 1988. Replication of the poliovirus genome, p. 23–48. *In* E. Domingo, J. J. Holland, and P. A. Ahlquist (ed.), RNA genetics, vol. 1. CRC Press, Boca Raton, Fla.
63. **Sonenberg, N.** 1987. Regulation of translation by poliovirus. Adv. Virus Res. **33:**175–205.
64. **Steinhauer, D. A., and J. J. Holland.** 1987. Rapid evolution of RNA viruses. Annu. Rev. Microbiol. **41:**409–433.
65. **Strauss, J. H., and E. G. Strauss.** 1988. Evolution of RNA viruses. Annu. Rev. Microbiol. **42:**657–683.
66. **Studier, F. W., and B. A. Moffat.** 1986. Use of bacteriophage T7 RNA polymerase to direct selective high-level expression of cloned genes. J. Mol. Biol. **189:**113–130.
67. **Studier, F. W., A. H. Rosenberg, J. J. Dunn, and J. W. Dubendorff.** 1990. Use of T7 RNA polymerase to direct the expression of cloned genes. Methods Enzymol. **185:**60–89.
68. **Thukral, S. K., M. L. Morrison, and E. T. Young.** 1991. Alanine scanning site-directed mutagenesis of the zinc fingers of transcription factor ADR1: residues that contact DNA and that transactivate. Proc. Natl. Acad. Sci. USA **88:**9188–9192.
69. **Traynor, P., B. M. Young, and P. Ahlquist.** 1991. Brome mosaic virus 2a protein: effects on RNA replication and systematic spread. J. Virol. **65:**69–77.
70. **Trono, D., R. Andino, and D. Baltimore.** 1988. An RNA sequence of hundreds of nucleotides at the 5′ end of poliovirus RNA is involved in allowing viral protein synthesis. J. Virol. **62:**2291–2299.
71. **Tuschall, D. M., E. Hiebert, and J. B. Flanegan.** 1982. Poliovirus RNA-dependent RNA polymerase synthesizes full-length copies of poliovirion RNA, cellular mRNA, and several plant virus RNAs in vitro. J. Virol. **44:**209–216.
72. **van der Werf, S., J. Bradley, E. Wimmer, F. W. Studier, and J. J. Dunn.** 1986. Synthesis of infectious poliovirus RNA by purified T7 RNA polymerase. Proc. Natl. Acad. Sci. USA **83:**2330–2334.
73. **Van Dyke, T. A., and J. B. Flanegan.** 1980. Identification of poliovirus polymerase P63 as a soluble RNA-dependent RNA polymerase. J. Virol. **35:**733–740.
74. **Wahba, A. J., M. J. Miller, A. Niveleau, T. A. Landers, G. G. Carmichael, K. Weber, D. A. Hawley, and L. I. Slobin.** 1974. Subunit I of Qβ replicase and 30S ribosomal protein S1 of *Escherichia coli*. Evidence for the identity of the two proteins. J. Biol. Chem. **249:**3314–3322.
75. **Ward, C. D., M. A. Stokes, and J. B. Flanegan.** 1988. Direct measurement of the poliovirus RNA polymerase error frequency in vitro. J. Virol. **62:**558–562.
76. **Wertman, K. F., D. G. Drubin, and D. Botstein.** 1992. Systematic mutational analysis of the yeast ACT1 gene. Genetics **132:**337–350.
77. **Wu, S.-X., P. Ahlquist, and P. Kaesberg.** 1992. Active complete in vitro replication of nodavirus RNA requires glycerophospholipid. Proc. Natl. Acad. Sci. USA **89:**11136–11140.
78. **Ypma-Wong, M. F., P. G. Dewalt, V. H. Johnson, J. G. Lamb, and B. L. Semler.** 1988. Protein 3CD is the major poliovirus proteinase responsible for cleavage of the P1 capsid precursor. Virology **166:**265–270.